

INVESTIGATIONS INTO INVERSION OF MAGNETIC AND GRADIENT MAGNETIC DATA FOR DETECTION AND DISCRIMINATION OF METALLIC OBJECTS

Dr. R. W. Groom, PetRos EiKon, Concord, Ontario, Canada
Dr. Ruizhong Jia, PetRos EiKon, Concord, Ontario, Canada
Dr. Catalina Alvarez, PetRos EiKon, Concord, Ontario, Canada

Abstract

We have extended our three-dimensional magnetic modeling capabilities to simulate TMI, magnetic vector and gradient measurements for both permanent magnetization and strong induced effects. We have developed capabilities to model quite general 3D shapes including conical and cylindrical objects both solid and hollow. These general shapes can be combined to represent projectile shells with quite general shapes having varying internal magnetic properties.

With these simulation capabilities, we investigated the use of inversion algorithms to determine the internal magnetization vector of buried objects. Our objectives are to understand the limitations of recovering the location of the magnetization vector as well as its magnitude and vector orientation. Determining the strength and orientation of the internal magnetization can help in the discrimination of material properties. Our experiments include examination of data sampling, data noise and combinations of TMI, vector and gradient measurements to resolve the magnetization. As an example, we determined that with adequate data sampling one could determine, extremely accurately, the location and orientation of the internal magnetization vector only if the volume of the object is known. This was accomplished by non-linear inversion combined with iterative grid volume modification. In addition, we have experimented with the use of a modified Euler deconvolution technique for depth estimation. At present, we are working with combining the two techniques.

Introduction

To investigate imaging, inversion and discrimination of metallic objects within the ground with the use of magnetic data collected on the surface, we decided to proceed first by developing the ability to simulate magnetic measurements from such objects. Traditionally, magnetic fields are simulated by the assumption that internal magnetization in the object is parallel to the earth's field and proportional to the susceptibility contrast. Often, the simulation assumes a two-dimensional geometry for the magnetic objects. For the purposes of UXO targets, of course, these assumptions are by no means sufficient. We, therefore, have proceeded on several fronts to implement more comprehensive simulation capabilities.

First, we have developed the ability to simulate non-linear induced magnetization effects for 3D objects. This is important as the metallic objects can have very large susceptibilities and in such cases there are a number of observed non-linear effects. These effects include both the so-called "demagnetization effect" or saturation effects and magnetic channelling effects. Second, we have added the ability to simulate permanent magnetic effects which are common in 3D metallic objects as well as the combination of permanent and induced magnetic effects. Thirdly, we have developed the ability to simulate projectile style geometries as well as landmine geometries for both non-linear, linear and permanent magnetic effects. Fourthly, we wished to simulate the derivatives of the magnetic field more

accurately than by taking spatial finite-difference estimates. We therefore implemented for all physical factors (linear, non-linear and permanent) solutions for the derivatives through quasi-analytic extensions of the solving techniques. Finally, we wished to incorporate the possibility of interactions between metallic objects. This, of course, is particularly important when a single object consists of multiple regions with different magnetic properties. In this case, the response of the objects may not be simply the addition of the different portions as there may be interactions between the different regions. For example, the induced field inside one region from the permanent magnetization of another region.

With these simulation capabilities, we were then able to begin the study of attempting to determine size, orientation, depth-of-burial and magnetic characteristics of metallic objects through inversion and imaging techniques.

Forward Simulation of Metallic Objects

Non-linear and linear induced magnetization

We briefly describe an algorithm to evaluate the magnetic field of a buried object. Given an magnetic anomaly V with magnetic distribution $\mu(\mathcal{F})$, immersed in background of constant electromagnetic properties, the magnetic field is described by

$$H(\mathcal{F}) = H_b(\mathcal{F}) + \iiint_V d\mathcal{F}' \overline{G}(\mathcal{F}, \mathcal{F}') Q(\mathcal{F}') H(\mathcal{F}') \quad (1)$$

where $Q(\mathcal{F}) = \mu^*(\mathcal{F}) - \mu_b^*$ and $\overline{G}(\mathcal{F}, \mathcal{F}')$ is the Green's tensor. Assuming that the magnetic field inside the integral can be approximated with its respective value at observation point, equation (1) can be written via the Nonlinear Approximator technique (Habashy, Groom and Spies, 1993)

$$H(\mathcal{F}) = H_b(\mathcal{F}) + L(\mathcal{F})H(\mathcal{F})$$

where

$$L(\mathcal{F}) = \iiint_V d\mathcal{F}' \overline{G}(\mathcal{F}, \mathcal{F}') Q(\mathcal{F}') \quad (2)$$

A difficulty arises in evaluating this integral due to the singularity of the Green's tensor $\overline{G}(\mathcal{F}, \mathcal{F}')$ inside the region V . To resolve this issue we need to rewrite (2) as

$$H(\mathcal{F}) = H_b(\mathcal{F}) + \iiint_V d\mathcal{F}' \overline{G}(\mathcal{F}, \mathcal{F}') Q(\mathcal{F}') + L^*(\mathcal{F})H(\mathcal{F})$$

with

$$L^*(\mathcal{F}) = \iiint_V d\mathcal{F}' \overline{G}(\mathcal{F}, \mathcal{F}') [Q(\mathcal{F}') - Q(\mathcal{F})].$$

Now by partitioning the anomaly V into M small regions $dV(j)$, $1 \leq j \leq M$., we have

$$L^*(\mathcal{F}_j) = \sum_{j=1}^M \iiint_{dV(j)} d\mathcal{F}' \overline{G}(\mathcal{F}_j, \mathcal{F}') [Q(\mathcal{F}') - Q(\mathcal{F}_j)].$$

This way we have overcome the singularity problem in evaluating (1). This is the basic approach that we have taken. We have calibrated this technique in several ways. First, against a 2D finite-element strong magnetization formulation technique, second when the magnetization is small versus traditional weak or Born scattering models, thirdly against known geological and metallic objects. This technique generalizes to interactions both of weak and strong nature (Groom and Alvarez, 2002).

Permanent magnetization

For permanent magnetization, we implement a constant magnetization vector source throughout each region of the object and evaluate the field due to this magnetization by standard volume integration of the magnetization weighted by the appropriate Green's tensor.

Polyhedral Volume Grids

The above techniques are general and independent of the model primitive to be used. Initially, of course, we utilized simple rectangular prisms. The method is stable for prisms of arbitrary aspect ratios and thus even prisms can provide very useful simulation (modeling) results. However, we have implemented more general models by the use of our polyhedral grids. Below we illustrate some of the range of capabilities that this can provide.

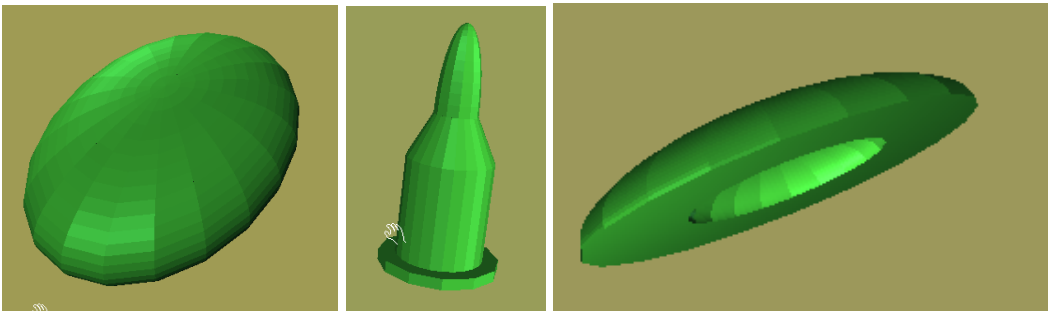


Figure 1.: Polyhedral Metallic Models

Formulation Test Results

As an illustration, we show some test results using the above mentioned forward formulation algorithms. The test was conducted with a solid and pipe of the same dimension:

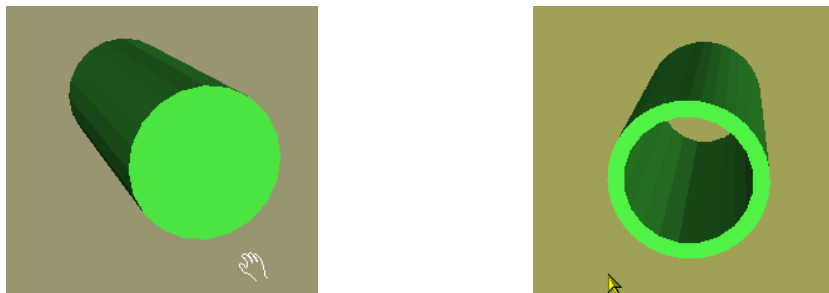


Figure 2.: Cylindrical Metal Objects:

Case 1: Solid (radius: 1m, length: 5m). Case 2: Hollow: inner radius 0.8 m, outer radius 1m, length 5m)

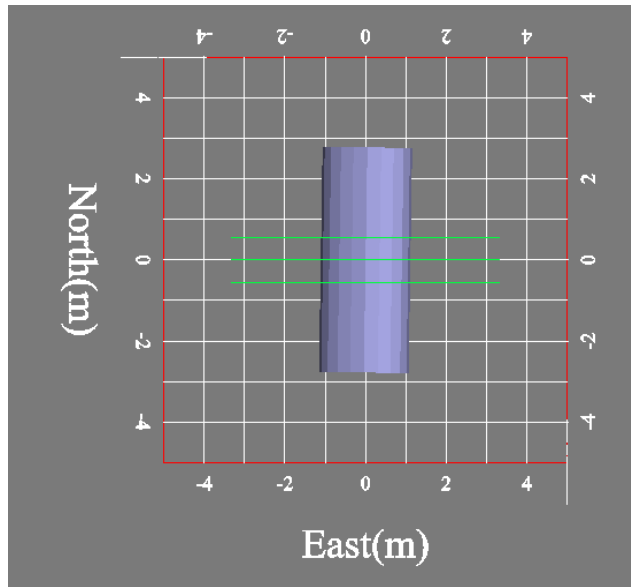


Figure 4.: Survey Geometry:

We show the total field magnetic response due to the susceptibility of the objects along the profile line across the center of the pipes. The solid pipe is shown as a blue curve and the hollow as red.

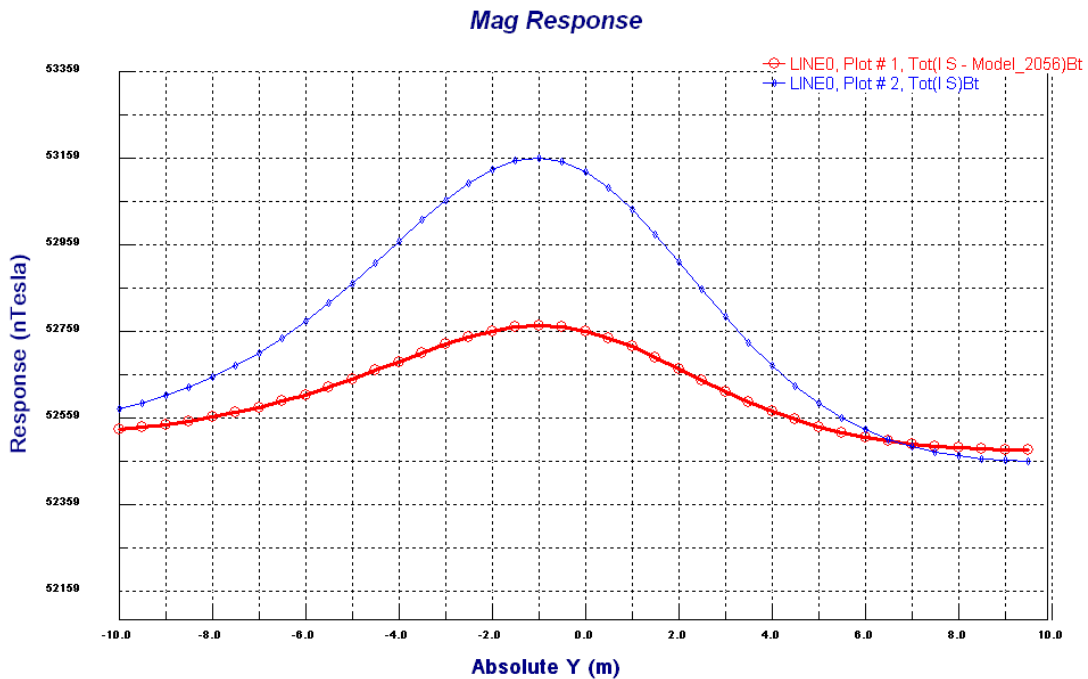


Figure 4. Simulated TMI from a solid cylinder and a pipe of same dimension.
 Red line: hollow pipe Blue line: solid cylinder

UXO Inversion Objectives

We give two inversion algorithms to detect buried magnetic objects.

Standard Least Squares Method for Magnetization Vector

This method applies to the case when only the amplitude of B-total field is measured. Let $\vec{M} = \vec{M}(\vec{r}')$ denote the magnetization density of the region in which the anomaly body is located. Then the scattered field due to the anomaly is given by

$$\vec{B}_s(\vec{r}) = \iiint_V G(\vec{r}, \vec{r}') \vec{M}(\vec{r}') d\vec{r}' ,$$

where V is the region of interest and $G(\vec{r}, \vec{r}')$ is Green's tensor.

Therefore the total field is

$$\vec{B}(\vec{r}) = \vec{B}_e + \vec{B}_s(\vec{r}) = \vec{B}_e + \iiint_V G(\vec{r}, \vec{r}') \vec{M}(\vec{r}') d\vec{r}' ,$$

where $\vec{B}_e(\vec{r})$ represents the earth's magnetic field.

To locate the magnetic source, we break the anomaly into M cells and assume that there exists exactly one cell having magnetization. The task is to identify the location of this specific cell, cell j say, and compute its magnetization (amplitude as well as direction. The information we have is that the amplitude of the total magnetic field is measured at N stations:

$$\left| \vec{B}(\vec{r}_1) \right| , \left| \vec{B}(\vec{r}_2) \right| , \dots , \left| \vec{B}(\vec{r}_N) \right| .$$

The problem can be formulated as

$$\left| \vec{B}(\vec{r}_i) \right| = \left| \vec{B}_e + G(\vec{r}_i, \vec{r}_j) \vec{M}_j \Delta V_j \right| , \quad i = 1, 2, \dots, N, \quad (1)$$

where $\vec{M}_j \Delta V_j$ stands for the volume magnetization of cell j , and \vec{r}_j specifies the location of the center of cell j . Cell j can be located by applying the standard least squares method. Upon achieving this, the nonlinear equation system (1) can be solved for the unknowns \vec{M}_j .

In this example, we have a small object (10cm x 10cm x 30cm), centered at a depth of 1m and inclined at 75 degrees to the horizontal and oriented to the SW at 45 degrees with a constant magnetization along its length with an amplitude twice the earth's field. We utilize three profiles of length 6m along the EW direction separated by 50cm with a data sampling every 20cm.

The following table illustrates our results. The first line indicates the objects center, the magnetization vector and the objects volume. The inverse results are based upon a search grid with constant cell size indicated the last column (in cubic metres). For the initial inversion, we search through the entire survey area and to a depth of 10m while for the remaining inversions, we utilized a 4x4m square to a depth of 2m, centered on the xy location indicated from the first inversion.

Table 1: Least Squares Inversion Results for Magnetization Vector

Model	X centre	Y centre	Z centre	Dip	Decl	Strength	Cell Size
Actual	-1	0.25	-1	75	225	2	0.003
Inverse I	-1.25	0.75	-0.75	33	-33	0.034	0.125
Inverse II	-1.1	0.3	-0.9	77	264	0.6	0.008
Inverse III	-0.95	0.25	-1	74.9	223	1.49	0.004
Inverse IV	-1.05	0.25	-0.95	76	235	1.8	0.003

Our experiments show over and over again that if the volume of the buried objective is known, its location as well as its magnetization vector can be well determined. Adequate data sampling and noise, of course, affect the accuracy of the results. This would imply that if a search was done for an object of known aspect ratio and volume then the objects depth and position could be accurately determined. If, in addition, the nature of its magnetization were known then the object could be discriminated.

Euler Deconvolutin

In the use of magnetic data for petroleum orientation, there is much use made of depth imaging techniques and structural index techniques such as the Wenner and Euler Deconvolution techniques.

For these techniques, we assume that the gradient of the B-total is known, the Euler deconvolution technique can be used to interpret any potential data in terms of depth and geological structure (see [3], [4]). Consider a magnetic source with center at (x_0, y_0, z_0) . For this source some total

magnetic field measurements $B(x_i, y_i, z_i)$ and its gradients $\frac{\partial B(x_i, y_i, z_i)}{\partial x_i}$, $\frac{\partial B(x_i, y_i, z_i)}{\partial y_i}$, $\frac{\partial B(x_i, y_i, z_i)}{\partial z_i}$ are made at locations (x_i, y_i, z_i) , $i = 1, 2, 3, \dots, m$. Let B represent the background field and

let

$$\Delta B(x_i, y_i, z_i) = B(x_i, y_i, z_i) - B.$$

Then ΔB satisfies Euler's equation:

$$(x_i - x_0) \frac{\partial \Delta B(x_i, y_i, z_i)}{\partial x} + (y_i - y_0) \frac{\partial \Delta B(x_i, y_i, z_i)}{\partial y} + (z_i - z_0) \frac{\partial \Delta B(x_i, y_i, z_i)}{\partial z} = -N \Delta B(x_i, y_i, z_i)$$

$i = 1, 2, 3, \dots, m$, where N stands for the structural index.

Differentiating $\Delta B(x_i, y_i, z_i) = B(x_i, y_i, z_i) - B$ gives

$$\frac{\partial \Delta B(x_i, y_i, z_i)}{\partial x} = \frac{\partial B(x_i, y_i, z_i)}{\partial x}$$

$$\frac{\partial \Delta B(x_i, y_i, z_i)}{\partial y} = \frac{\partial B(x_i, y_i, z_i)}{\partial y}$$

$$\frac{\partial \Delta B(x_i, y_i, z_i)}{\partial z} = \frac{\partial B(x_i, y_i, z_i)}{\partial z}.$$

Consequently,

$$\begin{pmatrix} \frac{\partial B(x_1, y_1, z_1)}{\partial x} & \frac{\partial B(x_1, y_1, z_1)}{\partial y} & \frac{\partial B(x_1, y_1, z_1)}{\partial z} \\ \frac{\partial B(x_2, y_2, z_2)}{\partial x} & \frac{\partial B(x_2, y_2, z_2)}{\partial y} & \frac{\partial B(x_2, y_2, z_2)}{\partial z} \\ \frac{\partial B(x_m, y_m, z_m)}{\partial x} & \frac{\partial B(x_m, y_m, z_m)}{\partial y} & \frac{\partial B(x_m, y_m, z_m)}{\partial z} \end{pmatrix} \begin{pmatrix} x_0 - x \\ y_0 - y \\ z_0 - z \end{pmatrix} = \begin{pmatrix} -N\Delta B(x_1, y_1, z_1) \\ -N\Delta B(x_2, y_2, z_2) \\ \Lambda \ \Lambda \ \Lambda \\ -N\Delta B(x_m, y_m, z_m) \end{pmatrix}$$

For a given N (structural index), the location of source (x_0, y_0, z_0) can be solved.

Euler deconvolution only estimates the location of the internal magnetization vector of buried objective. Gradients and total field have to be provided for this technique. Once the location of the magnetization vector is known, we may use the first method to determine its strength as well as orientation without doing iterative grid volume modification. This will be treated in our future work.

References

- [1] T. M. Habashy, R. W. Groom and B. R. Spies, Beyond the Born and Rytov Approximations: A Nonlinear Approach to Electromagnetic Scattering, JGR, 98, no. B2, (1993).
- [2] R. W. Groom and C. Alvarez, 3D EM modelling – Application of the Localized Non-linear Approximator to near surface applications, SAGEEP Meeting, (2002).
- [3] Jeffrey D. Phillips, Two-step processing for 3D magnetic source locations and structural indices using extended Euler or analytical signal methods, SEG International Exposition and 72nd Annual Meeting, 2002.
- [4] Changyou Zhang, Martin F. Mushayandebvu, Alan B. Reid, J. Derek Fairhead, and Mark E. Odegard, Euler deconvolution of gravity tensor gradient data, Geophysics, Vol. 65, NO.2, P.512-520, 2000.